Déformations induites des renforts fibreux pré-imprégnés en consolidation : Étude expérimentale et modélisation

Experimental study and modeling of flow-induced deformations of continuous prepregs during consolidation

Alexandre Hautefeuille[1] et Sébastien Comas-Cardona[1]

1 : Équipe Procédés et Mécanique des Matériaux (PMM), Institut de Recherche en Génie Civil et Mécanique (GeM)
UMR CNRS 6183, École Centrale de Nantes
1 rue de la Noë, 44300 Nantes
e-mail : alexandre.hautefeuille@ec-nantes.fr

Résumé

La mise en forme des matériaux composites à matrice thermoplastique au moyen de procédés à haute cadence engendre un fort couplage hydromécanique entre la matrice et le renfort de fibres continues. De nouveaux mécanismes de grandes déformations de l'architecture fibreuse apparaissent lorsque l'écoulement généré a la capacité d'emporter avec lui le milieux fibreux. Cette étude met en évidence le phénomène de transport de fibres lors de la consolidation transverse du composite et introduit la déformation induite du milieu fibreux dans la modélisation du procédé.

Mots Clés : Consolidation, Déformations induites, Suivi de procédé

Abstract

The processing of thermoplastic matrix composites with high speed processes results in a strong hydro-mechanical coupling between the matrix and the continuous fibre reinforcement. New mechanisms of large deformations of the fibrous architecture then appear when the generated flow has the capacity to carry the fibrous medium. This study highlights the phenomenon of fibre tows transport (also called fibre washout) during the transverse consolidation of the composite and introduces the induced deformation of the fibrous medium into the process modelling.

Keywords : Composite consolidation, Flow-induced deformations, Process monitoring

1. Introduction

Consolidation is an inherent step in various processes for shaping composite materials (Consolidation of prepregs by autoclave, C-RTM, compression of discontinuous plies...). These processes, controlled by transverse compression at high temperature, consist in shaping a fibrous reinforcement from different plies of fabrics pre-impregnated with an organic matrix. When these different plies of prepreg fabrics are subjected to the transverse consolidation force, a flow of the matrix (fluid at process temperature) can be generated in the plane. This flow allows the saturation of the fibrous medium with the matrix by expelling the air initially present in the fibrous medium porosity content. The consolidation phase is completed when the now saturated fibrous medium reaches the volume fibre content defined for the final part. The hydro-mechanical coupling generated by the consolidation of the saturated fibrous reinforcement can induce two different kind of in-plane flow. When the fluid stress is lower than the cohesion forces of the fibrous structure, the flow is carried out through the fibrous medium, which remains static in the plane, and guarantees the manufacturing of structural composite parts whose fibrous orientation is fixed. This is called a filtration or bleeding flow. However, when the fluid drag force becomes greater than the cohesion forces of the fibrous structure, the flow has the ability to move the fibre tows of the reinforcement, modifying the fibrous architecture and the orientations of the tows of the final part. Therefore, the hydro-mechanical mechanisms related to consolidation must be controlled because they play a crucial role in the quality of the composite part produced.

2. Highlighting of the in-plane washout phenomenon during consolidation

The phenomenon of flow-induced deformation can be demonstrated by adding metallic wires to the fibrous architecture. After the consolidation of the composite material, the analysis of the position of these wires will show the deformed state of the fibrous architecture.

2.1. Sample preparation

A quasi-unidirectional fabric (Chomarat UDT400P, 420g/m^2) is used a raw material in this study. The fibrous reinforcement is made with 6 rectangular fabric plies (90x75 mm). As indicators of de deformation, thin copper wires with 0.1 mm diameter are added within each ply with a constant step as illustrated in Figure 1. The Figure 2 presents a microscopy of a copper wire added within the fibrous architecture. The copper wire is woven within the fibrous architecture itself, which forces it to follow the deformation kinematics of the fibre tow.

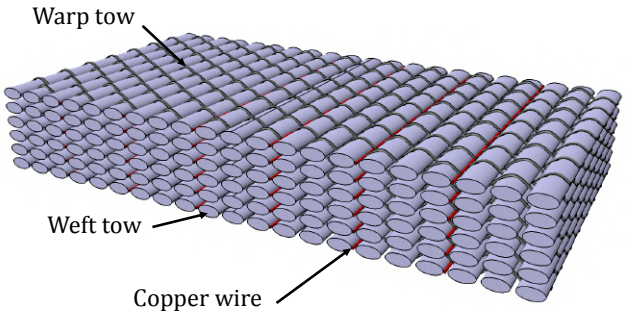

Fig. 1. Sample scheme

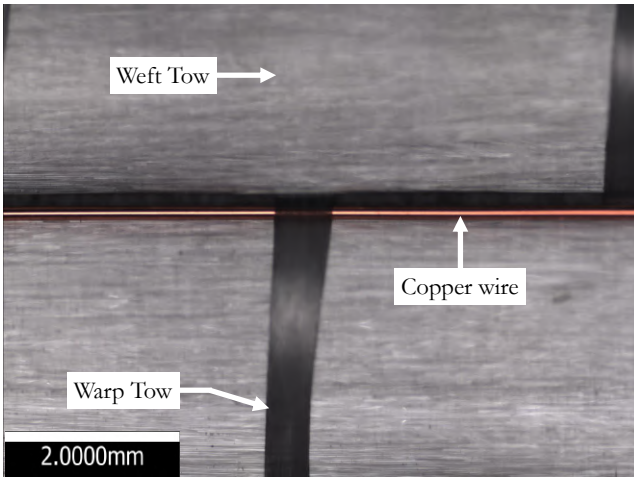

Fig. 2. Microscopy of the copper wire inserted within the fibrous architecture

Then the dry fibrous reinforcement is impregnated with an epoxy resin as matrix (Loctite EA 9396 Aero, viscosity during impregnation : μ =3.5 Pa.s) and then consolidated under 200 kN at 70°C.

2.2. Deformation analysis

A tomographic analysis of the consolidated sample is realized using a Bruker SkyScan 1275 with a 50 μm scaled image voxel size. An isometric view of the 3D X-ray tomography is presented in Figure 3.

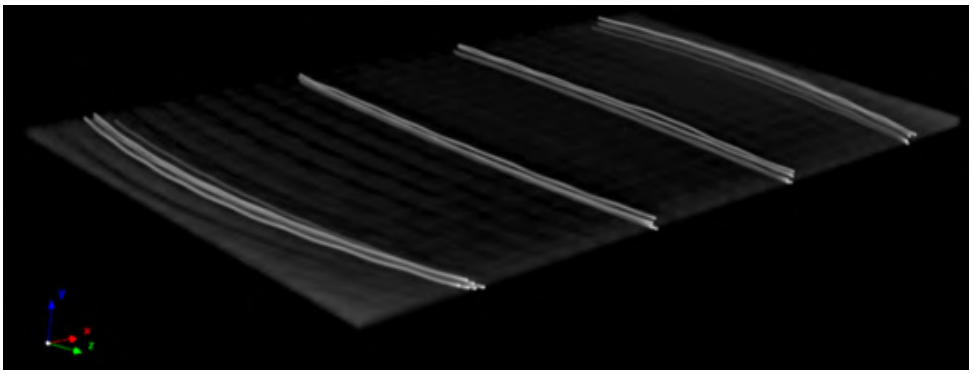

Fig. 3. CT-scan of the consolidated sample (Resolution : 1 Px=50 um)

After reconstruction, a Matlab algorithm computes for every sample slice each single copper wire displacement and both the mean displacement and the standard deviation of the four copper wire group presented in Figure 3. The following Table 1 summarizes the results obtained by the post-treatment.

Tab. 1. Measurements of copper wires displacement

Copper wire group	Measured mean displacement (mm)	Standard deviation (mm)
Group n°1	5.9	1.3
Group n°2	1.9	0.5
Group n°3	1.3	0.4
Group n°4	5.5	1.1

From those results, one can sense that the deformation increases with the distance to the center of the sample center. Moreover, the deformation appears to be frontal. Indeed, the low standard deviation indicates that each ply presents almost the same deformation. From those results, the hypothesis that the in-plane deformation of the whole fibrous reinforcement can be observed looking at a single-ply deformation is taken.

3. Real-time monitoring of flow induced in-plane deformation

3.1. Experimental set-up for a local study of in-plane washout

A large-scale semi-transparent test bench has been developed in order to continuously track the in-plane motion of the fiber-tows occurring during a saturated compression. The setup, presented in details in [1], allows the compression of samples up to 400 mm side length under 200 kN maximal compressive force. In order to perform the image processing, uv-reactive markers are placed on the ply in contact with the bottom transparent platen. Figure 4 illustrates the principle of the experiment and Figure 5 presents a photography taken during the consolidation of a fibrous reinforcement with a uv-reactive fluid as matrix.

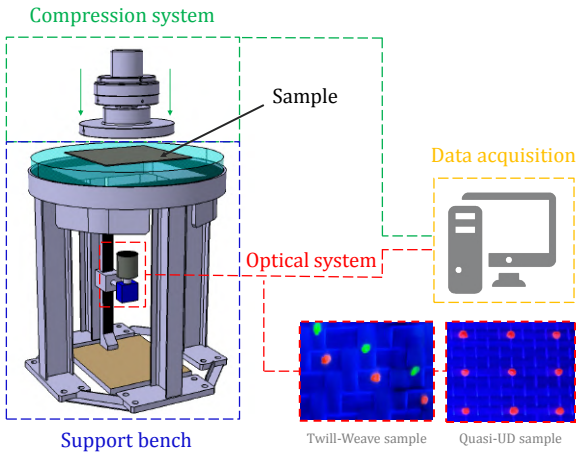

Fig. 4. Principle of the experiment

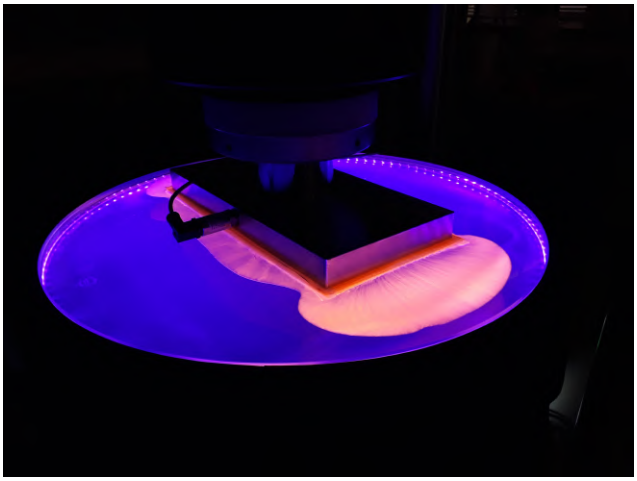

Fig. 5. Consolidation experiment in progress

3.2. Experimental investigations on an anisotropic fibrous reinforcement

As previously discussed, two kind of in-plane flow can arise from the consolidation of a composite : a bleeding flow or a fibre convecting flow. In this section, two experiments will be presented. While the first experiment encapsulates the process-material parameters linked to a bleeding flow, the second one generates a fibre convecting-flow. Table 2 presents the material and process parameters used for the experiments.

Tab. 2. Experimental parameters

Parameter	Exp.1	Exp.2
Fibrous reinforcement	UDT400P $[90]_6$	UDT400P $[90]_6$
Compression Platen	L=360 × l=180mm	L=360 × l=180mm
Compression speed	1.5 mm/min	1.5 mm/min
Fluid viscosity	0.09 Pa.s	4.58 Pa.s

Displacement field computation

An in-house algorithm has been developed in order to compute the in-plane displacement field of the fibre tows of the reinforcement during the transverse consolidation. This algorithm employs tracking and registration techniques for the measurement of the displacement of a particle-cloud (represented by the UV-reactive markers added to the fibrous architecture) between two images. In addition, the movement and the shape of some of the fibre tows can be found and displayed from the displacement of the markers painted on them. The following Figure 6 presents the displacement field and the shape of recognized fibre tows of the sample during the consolidation, at several steps of the latter, for Exp.1 and Exp.2. In the figure, the dashed line represents the boundary of the compression platen applying the compression stress on the top face of the sample. The corresponding fibre volume fraction, normal force and applied stress are also mentioned in the bottom-right corner.

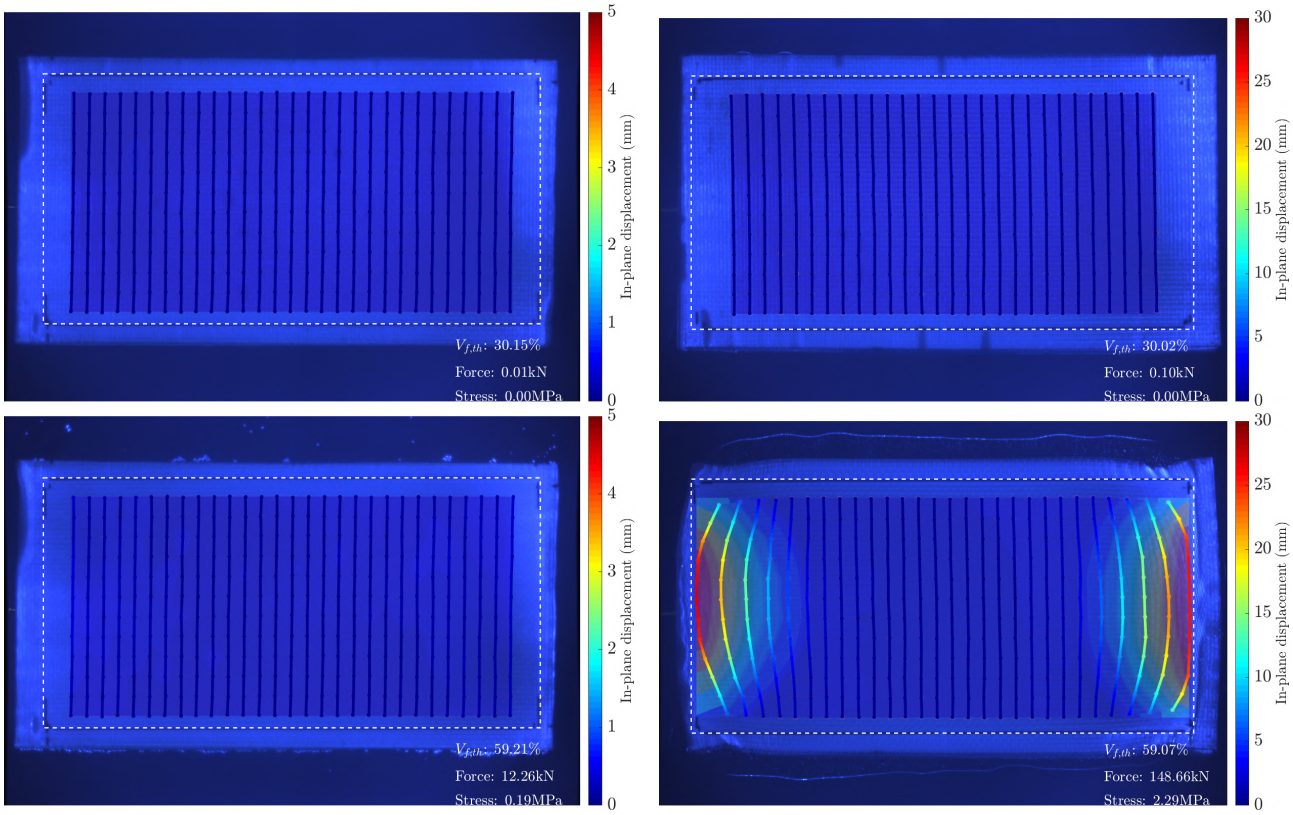

Fig. 6. In plane displacement field computed for Exp.1 (left) and Exp.2 (right) at V_f = 30% and V_f = 59%

These results confirm the increase of the displacement of the fibre tows with their distance to the centre of the part, this displacement is indeed due to the viscous drag force which increases with the pore velocity of the fluid [2]. This velocity, in a saturated flow regime, increases with the distance to the center of the part during consolidation. In addition, it can be seen that the deformation of the fibrous medium is transverse to the direction of the fibre tows, the latter being logically considered as

inextensible along their lengths (the fluid stress generated by the flow is negligible comparatively to the modulus of elasticity of the fibre).

Deformation field computation

At the macro-scale, the displacements of the tow induces in-plane deformations of the fibrous architecture. From the registred point-cloud displacement, one can derive the Green strain tensor of the deformable mesh based on the markers. With constant strain triangles and first order shape functions use [3], the Green strain tensor of the fibrous architecture is obtained. Figure 7 illustrates the generation of a triangular deformable mesh from Raw images.

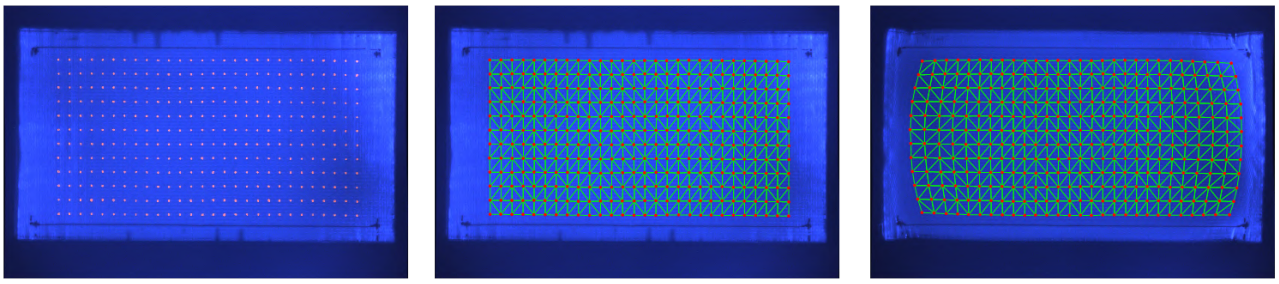

Fig. 7. Triangular deformable mesh generation

The Green strain tensor, **E**, is based on the deformation gradient as described in the following equation (Eq. 1) :

$$\mathbf{E} = \frac{1}{2}\left(\mathbf{F}^T \cdot \mathbf{F} - \mathbf{I}\right) \qquad F_{ij} = \delta_{ij} + \frac{\partial u_i}{\partial X_j} \tag{Eq. 1}$$

Where **F** is the transformation **u** gradient and **I** the identity. In 2D, the tensorial expression of the Green strains writes :

$$\mathbf{E} = \begin{bmatrix} E_{xx} & E_{xy} \\ \\ E_{xy} & E_{yy} \end{bmatrix} \tag{Eq. 2}$$

E_{xx} and E_{yy} being respectively the fibre tows transverse direction and the fibre tow direction. E_{xy} is the shear strain. This strain tensor is well suited for the washout phenomenon because its computation eliminates the rigid body rotation, so the strain of each element can be computed regardless of the rotation. In addition, as the small strain hypothesis is not applicable to this range of deformations, the strain tensor not only reduces to small strain terms but the quadratic terms have to be also taken in account. In order to define an equivalent strain, one can compute the euclidean norm of the Green strain tensor such as :

$$E_{eq} = \sqrt{\sum |E_{i,j}|^2} = \sqrt{E_{xx}^2 + 2E_{xy}^2 + E_{yy}^2} \tag{Eq. 3}$$

Figure 8 presents the equivalent deformation field (E_{eq} of the sample during the consolidation, at different compaction levels, for Exp.1 and Exp.2. In the figure, the dashed line represents the boundary of the compression platen applying compression stress on the top face of the sample.
The in-plane deformation of the sample introduces a local modification of the geometric properties of the material such as the fibre volume fraction and the permeability tensor. The following section emphasizes the consideration of in-plane deformations in the resolution of consolidation equation.

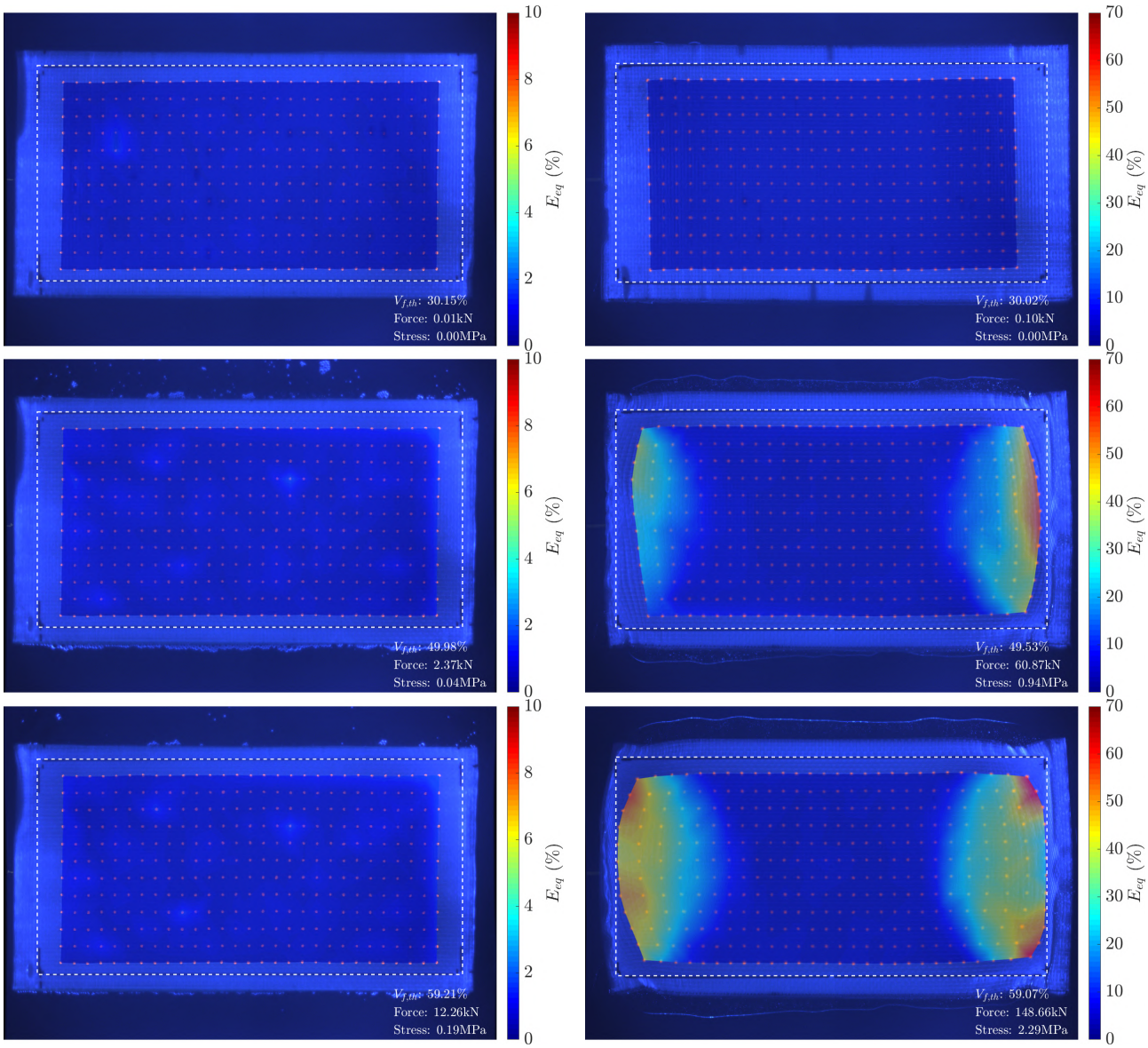

Fig. 8. Equivalent deformation field E_{eq} computed for Exp.1 (left) and Exp.2 (right) at $V_f = 30\%$, $V_f = 50\%$ and $V_f = 59\%$

4. Modeling

For continuous transverse compression of a saturated porous media, the fluid pressure is governed by the continuity equation combined with Darcy's law [4]. Assuming that the flow only occurs in the plane, and along the two principal flow direction (i.e neglecting K_{xy} terms) it writes in cartesian coordinates (x,y) :

$$K_x \frac{\partial^2 p}{\partial x^2} + K_y \frac{\partial^2 p}{\partial y^2} = -\mu \frac{\dot{h}}{h} \qquad \text{(Eq. 4)}$$

where K_x and K_y are the permeability tensor components in the main flow directions, p the fluid pressure, μ the fluid viscosity, $\dot{h}$ the compaction velocity, and h the thickness. The introduction of local geometric modifications of the fibrous architecture during consolidation requires the consideration of a new local volume fraction based on the deformations presented above. Thus, the global consolidation equation can be localized such as :

$$\mathbf{K_x}(x,y) \frac{\partial^2 p}{\partial x^2} + \mathbf{K_y}(x,y) \frac{\partial^2 p}{\partial y^2} = -\mu \frac{\dot{h}}{h} \qquad \text{(Eq. 5)}$$

where $\mathbf{K_x}(x, y)$ and $\mathbf{K_y}(x, y)$ are the local components of the permeability tensor. Thus, the permeability tensor is also modified by the decrease or increase of the local fibre volume fraction as presented in Figure 9.

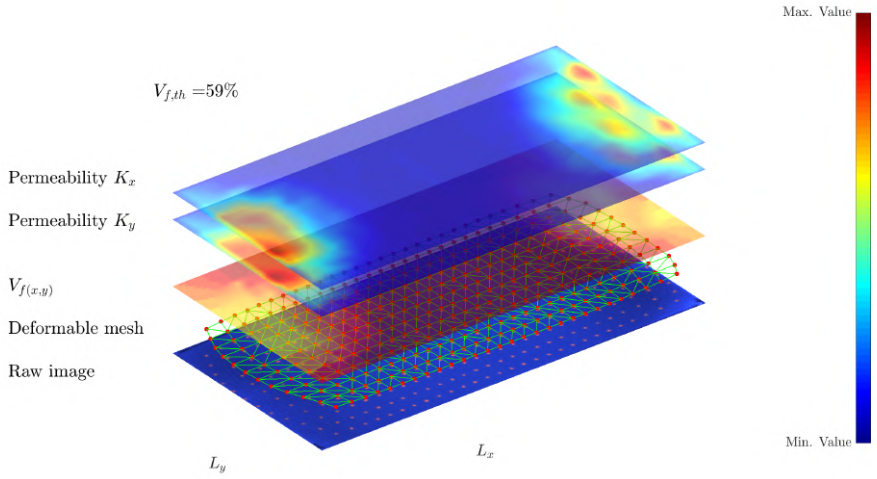

Fig. 9. Non-dimensionalized geometrical properties ($V_f(x, y)$, $K_x(x, y)$, $K_y(x, y)$ of the fibrous material evaluated at the average V_f = 59% for Exp.2.

Then, integrating the pressure field on the compression surface, one can retrieve de fluid force. Figure 10 presents the comparison of the experimental fluid force, the integrated consolidation pressure equation (Eq. 4) and the localized one (Eq. 5) proposed in this study, for Exp.1 and Exp.2.

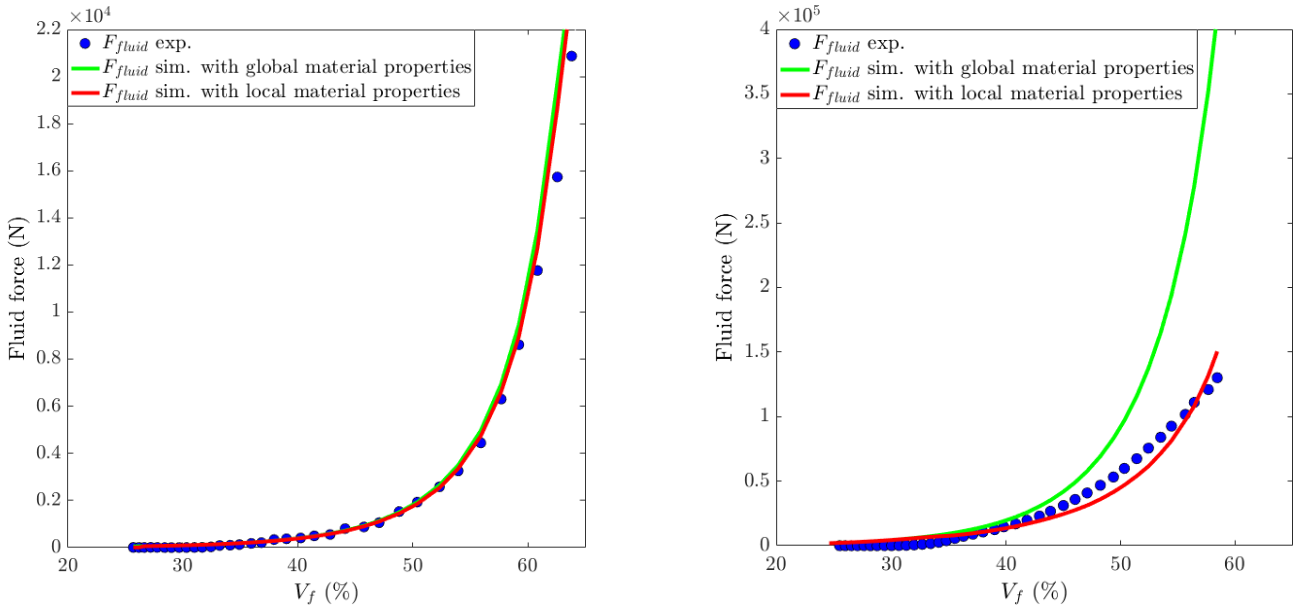

Fig. 10. Comparison between pressure experimental results and integrated (Eq. 4) *and* (Eq. 5) *for Exp.1 and Exp.2.*

From those results, one can sense that the modification of the consolidation equation does not introduce significant changes for Exp.1 because the in-plane deformation of the fibrous material is very limited during the experiment. However, as Exp.2 reveals a high in-plane deformation of the fibrous architecture, the consideration of new local geometrical properties brings the consolidation equation closer to experimental results.

5. Conclusion

This study highlights the washout phenomenon. Experimental results have shown that the latter is of a constant nature in the thickness of the part (when the consolidation addresses thin parts). From this point, the design of rich experiments paves the way to take into account the local deformations of fibrous architecture during consolidation. Therefore, the geometric parameters of the fibrous material can be reassessed during the process and introduced in the consolidation modelling. Then, an evaluation of local pressure gradients allows to quantify the viscous drag forces. The latter are directly opposed to the intrinsic cohesion mechanisms of the fibrous material. The current work therefore aims to evaluate these friction forces on a continuous basis during consolidation.

Acknowledgements

Part of this study is funded by FUI-AAP20 Regions Projects (France) within the INCREASE project (partners : Solvay, IFTH, Billion SAS, Pernoud, Chomarat Textiles Industries, IPC, INSA Lyon and Centrale Nantes). The authors would also like to thank Emmanuel Ormea of Synergie 4 for the production of tomographic images related to this work.

Références

[1] A. Hautefeuille, S. Comas-Cardona, C. Binetruy « Mechanical signature and full-field measurement of flow-induced large in-plane deformation of fibrous reinforcements in composite processing », *Composites Part A : Applied Science and Manufacturing* Vol. 118, pp. 213–222, 2019.

[2] C. Tucker, R. B. Dessenberger, et al. « Governing equations for flow and heat transfer in stationary fiber beds », *Composite Materials Series* , pp. 257–257, 1994.

[3] T. R. Chandrupatla, A. D. Belegundu, T. Ramesh, C. Ray, Introduction to finite elements in engineering, vol. 10, Prentice Hall Upper Saddle River, NJ, 2002.

[4] T. G. Gutowski, T. Morigaki, Z. Cai « The consolidation of laminate composites », *Journal of Composite Materials* Vol. 21 n° 2, pp. 172–188, 1987.